International Core Journal of Engineering Volume 9 Issue 4, 2023
ISSN: 2414-1895 DOI: 10.6919/ICJE.202304_9(4).0030

Experimental Study on Gas-Paraffin Direct Contact Phase Change Storage Heat Transfer

Hegang Zhu, Xiaoni Qi, Xiaohang Qu, Chunhu Miao

School of Transportation and Vehicle Engineering, Shandong University of Technology, Shandong 255000, China

Abstract

Through temperature measurement and visualization experiments, the heat transfer characteristics and condensation phenomena in the heat transfer process were studied and analyzed by using gas as heat transfer fluid and gas directly entering the direct contact phase change energy storage device through the nozzle. Thermocouples at different positions in the accumulator can measure the internal temperature change of PCM. The results show that the condensation time of heated PCM decreases with the increase of the flow rate of injected gas, and the maximum reduction of condensation time in the experiment is 24.36 %. The larger the nozzle, the lower the condensation time, but most cases are below 1 % ; the volume of paraffin in the phase transition increases with the increase of gas flow rate, and the volume increases by 275 % at the gas flow rate of 1.7 L / min. The heat transfer power was obtained by numerical calculation. With the increase of gas flow rate, the heat transfer power increased by 31.99 %. The development of direct contact phase change storage system achieves higher energy storage efficiency, higher heat release rate and simpler structure than traditional phase change storage system.

Keywords

Heat Transfer Fluid; Phase Change Energy Storage; Direct Contact; Heat Transfer Process; Visual Experiment.

1. Introduction

In the era of energy crisis, traditional fossil energy is not renewable, the use of phase change materials phase change latent heat for energy storage is a phase change energy storage technology widely used in the field of new energy development and building energy conservation. In view of the low thermal conductivity and poor heat transfer performance of organic phase change materials, many measures have been proposed to enhance heat transfer. Das et al. studied the effects of adding different volume fractions of graphene thermal conductivity materials to n eicosane on the performance of the heat accumulator, and found that when the temperature of the hot fluid was 60℃ and 70℃, adding 2% volume fraction of graphene could shorten the heat storage time by 41% and 37%, respectively [1]. Motahar et al. added titanium dioxide nanoparticles to n-octadecane phase change material and found that adding 3% titanium dioxide nanoparticles could increase the thermal conductivity of n-octadecane by about 5% [2]. The influence of tank structure and fin structure on heat transfer performance of phase change storage system in indirect vessel is studied. Mao found that the truncated cone with a taper of 0.37 has the best performance in the charging and discharging process, and the fin with a dip Angle of 15° has the most significant enhancement effect [3].Stritih[4] studied the influence of fins on the performance of phase-change energy storage heat exchanger through experiments and found that the energy release time of phase-change energy storage heat exchanger could be reduced by 40% by adding high-guide fins.

ISSN: 2414-1895 DOI: 10.6919/ICJE.202304_9(4).0030

Compared with the indirect container, the structure of the direct contact container is extremely simple, the heat transfer speed is fast, and the heat exchange tube can be ignored [5,6]. In vessels in direct contact, PCM is directly mixed with heat transfer fluids (HTFS), such as paraffin/water, concrete/water systems, etc. [7-9]. Huang et al. [10] studied the influence of fluid flow on heat transfer performance in the direct contact heat transfer process based on the EMD-LSSVM model, and the results showed that the proposed hybrid model could improve the prediction accuracy of volumetric heat transfer coefficient. He[11] et al. studied the enhanced heat transfer and melting behavior of phase change materials in direct contact energy storage vessels, and found that the melting process of phase change materials can be divided into forming channel stage, melting stage and final stage. Martin Belusko[12] et al. studied direct contact phase change material energy storage. Mechanical design requirements and pumping loss are the most critical factors for the development of direct contact PCM heat storage system. Wang[13] et al. studied the numerical simulation of the heat release process of the direct contact phase change energy storage system, and obtained the results of the influence of flow rate and inlet temperature on the performance of heat exchange oil. Sven Kunkel et al. proposed a new direct contact latent heat storage concept and obtained the heat transfer coefficient between oil and solid or molten phase change materials [14]. Current researches mainly focus on indirect contact energy storage vessels and improving the heat transfer coefficient of phase change materials. For direct contact energy storage vessels, most of the research focuses on heat transfer oil as heat transfer fluid, and there are no reports on the use of air as heat transfer fluid and the study of PCM temperature change and condensation form. In this paper, a new type of direct contact energy storage vessel is designed, which uses air as a heat transfer fluid. The temperature change and condensation form of PCM in the condensation process of direct contact energy storage are recorded by the camera and thermocouple. The temperature curve and condensation form diagram in the condensation process of PCM are obtained, as well as the heat transfer characteristics.

2. Experimental System and Method

The experimental system is shown in Figure 1. The air enters the experimental system through the air compressor, and then flows successively through the pressure stabilizer tank, filter pressure limiting valve, mass air flowmeter and nozzle before entering the experimental section. In order to ensure the constant heating temperature of paraffin wax, constant temperature heating plate and temperature controller are used to set the temperature value, and the heated liquid paraffin wax is quickly poured into the energy storage tank. In order to ensure the constancy of the intake temperature, keep the indoor temperature between 25℃. The upper half of the test section is a transparent acrylic container with an inner diameter of 70mm and a height of 130mm, and the lower half is a stainless steel container with an inner diameter of 70mm and a height of 30mm. The stainless steel bottom is provided with M6 threads for the fixation of nozzles, and the upper and lower sections are connected by flanges.

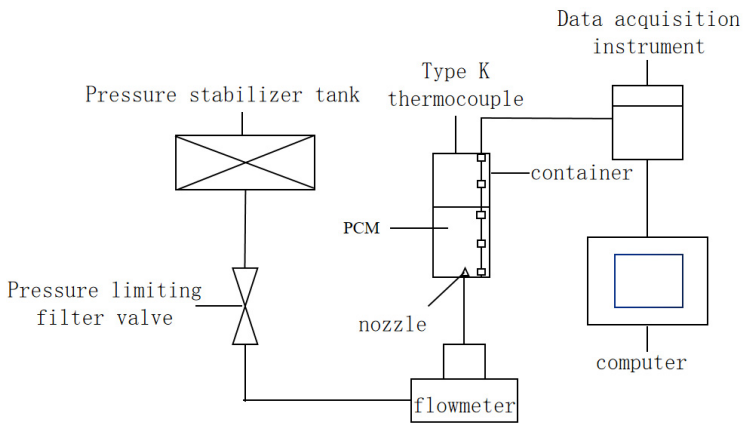

Fig 1. Experimental structure diagram

ISSN: 2414-1895 DOI: 10.6919/ICJE.202304_9(4).0030

K-type thermocouple is used in the experimental section and heating plate, and the control accuracy is 1℃. Five K-type thermocouples were arranged in different height positions in the test section container for temperature measurement, from the bottom to T1, T2, T3, T4, T5. The horizontal distance from the center point of the energy storage tank is 18mm, and the temperature accuracy of K-type thermocouple is 0.5℃ after temperature check. The air flowmeter is Asalt air mass flowmeter with a range of 0-5SLM, inlet pressure of 0.1Mpa and control accuracy of 0.5%. SMC AW30-02BG-B model is adopted for pressure limiting drying valve, which can automatically control the gas pressure within the required range and remove the moisture and impurities in the gas. The filtration accuracy is 5.0. Phase change material is No.58 fully refined paraffin wax, melting point at about 58℃. Because paraffin wax is amorphous, it has no specific melting point. The specific heat capacity is 3.20kJ·kg-1·K-1 in the solid state and 2.80kJ·kg-1·K-1 in the liquid state. The thermal conductivity is 0.35W·m-1·K-1 in the solid state, and 0.15W·m-1·K-1 in the liquid state. The test conditions involved in this experiment, such as nozzle outlet diameter, paraffin mass, heating temperature and gas flow, are shown in Table 1, a total of 21 different test conditions.

Table 1. Test conditions

Nozzle diameter mm	Paraffintemperature ℃	Paraffin mass g	Air flow L/min
0	120	130	0
0.4	120	130	0.9,1.1 ,1.3,1.5,1.7
0.6	120	130	0.9,1.1 ,1.3,1.5,1.7
0.8	120	130	0.9,1.1 ,1.3,1.5,1.7
1.0	120	130	0.9,1.1 ,1.3,1.5,1.7

3. Data Processing

In order to obtain the temperature change curves of phase change materials under different conditions, Xunyan temperature acquisition module was used for acquisition, and the acquisition interval was 3s. The collected temperature change data is presented in the form of charts.

The gas directly enters the accumulator from the exit nozzle and contacts the PCM to generate forced convectio ansfer. After the air is filtered and dried, the impurities and moisture contained in the air can be removed, so the gas can be regarded as pure air. The temperature of PCM is taken as the average temperature of paraffin wax measured, so as to calculate the total enthalpy. Because the temperature of different positions inside the paraffin wax in the accumulator is different, it can be clearly seen from Figure 2 to Figure 6 that the temperature below the paraffin wax is high and the temperature above is low. For the PCM in the accumulator, the enthalpy of the solid phase, liquid phase and paste region is different. The enthalpy of the paste zone has both sensible heat and latent heat. It is not practical to measure the volume fraction or temperature field occupied by the liquid phas β e of the PCM in the accumulator. Therefore, in this study, the enthalpy change method without explicitly tracking the solution interface is used to estimate the instantaneous specific enthalpy. The total enthalpy (H) at a certain temperature is defined as the sum of sensible enthalpy (h) and latent enthalpy (ΔH), and h is the sum of the reference value h_{rer} and relative value h_{rel} of sensible enthalpy:

$$H = h + \Delta H = h_{ref} + \int_{T_{ref}}^{T} C_P dT + \Delta H \tag{1}$$

The content of latent enthalpy can vary between 0 (latent enthalpy of solid phase) and L (latent enthalpy of liquid phase), so ΔH can be expressed as:

$$\Delta H = \beta L \tag{2}$$

ISSN: 2414-1895 DOI: 10.6919/ICJE.202304_9(4).0030

Liquid phase ratio (β) is defined as:

$$\beta = \begin{cases} 0, & T < T_s \\ \dfrac{T - T_s}{T_l - T_s}, & T_s < T < T_l \\ 1, & T > T_l \end{cases} \tag{3}$$

After introducing the liquid phase rate, the equation can be written as a unified expression:

$$H = h + \Delta H = h_{ref} + \int_{T_{ref}}^{T} C_P dT + \beta L \tag{4}$$

The condensing heat transfer power of PCM is expressed as the ratio of the total enthalpy of PCM to the condensing time:

$$P = \frac{H}{t} \tag{5}$$

4. Experimental Results

4.1 Cooling Temperature and Time of Paraffin

The air flow rate is 0L/min, and the experimental data are shown in Figure 2. It takes 243 minutes and 33 seconds for the paraffin to cool to 30℃.

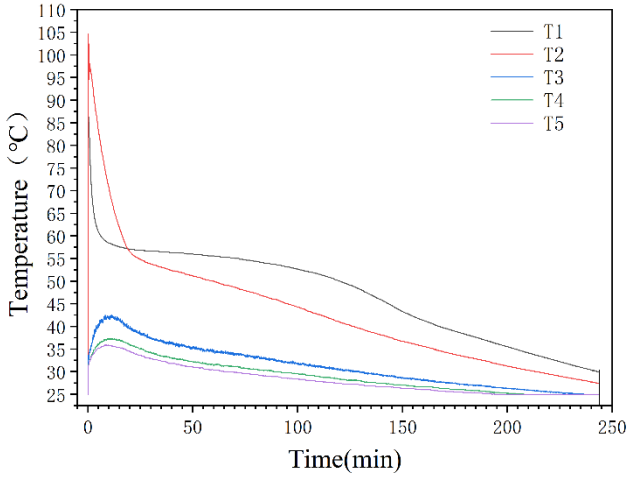

Fig 2. Temperature curve of paraffin without gas

The nozzle diameter is 0.4mm, and the air flow rate is 0.9L/min, 1.1L/min, 1.3L/min, 1.5L/min and 1.7L/min, respectively. Experimental data are shown in Figure 3. Under the condition of air flow of 0.9L/min, the cooling time of paraffin wax to 30℃ is 221 minutes 51 seconds; under the condition of air flow of 1.1L/min, the cooling time of paraffin wax to 30℃ is 213 minutes 39 seconds; under the condition of air flow of 1.3L/min, the cooling time of paraffin wax to 30℃ is 213 minutes 39 seconds. It takes 205 minutes and 57 seconds for the paraffin to cool to 30℃. Under the condition of air flow 1.5L /min, the cooling time of paraffin wax to 30℃ is 194 minutes 57 seconds, and under the condition of air flow 1.7L/min, the cooling time of paraffin wax to 30℃ is 187 minutes 18 seconds.

ISSN: 2414-1895 DOI: 10.6919/ICJE.202304_9(4).0030

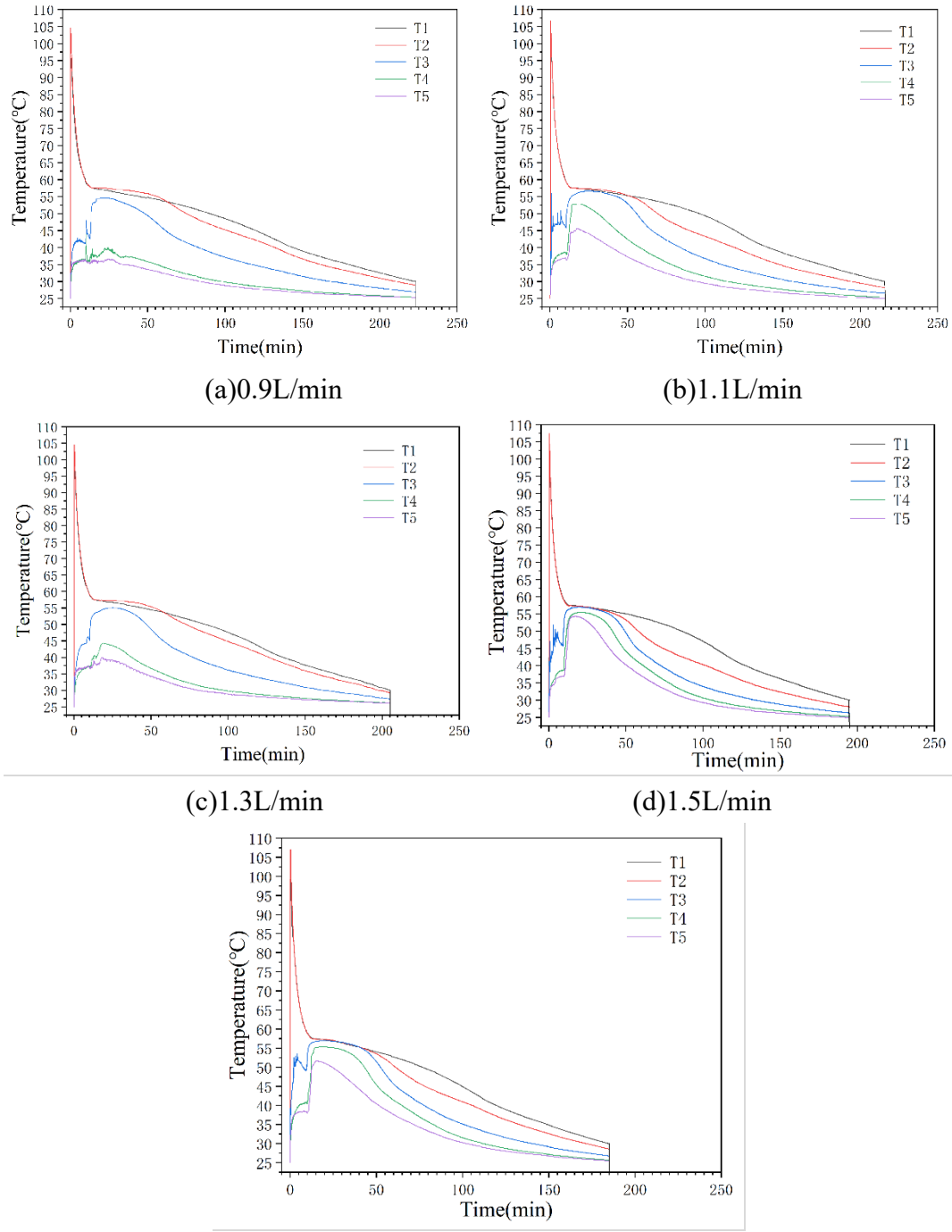

(a)0.9L/min (b)1.1L/min

(c)1.3L/min (d)1.5L/min

(e)1.7L/min

Fig 3. Temperature variation curve of 0.4mm nozzle paraffin

The nozzle diameter is 0.6mm, and the air flow rate is 0.9L/min, 1.1L/min, 1.3L/min, 1.5L/min and 1.7L/min, respectively. Experimental data are shown in Figure 4. Under the condition of air flow of 0.9L/min, it takes 219 minutes and 24 seconds for paraffin to cool to 30℃; under the condition of air flow of 1.1L/min, it takes 212 minutes and 12 seconds for paraffin to cool to 30℃; under the condition of air flow of 1.3L/min, It takes 203 minutes and 42 seconds for the paraffin to cool to 30℃. Under the condition of air flow 1.5L/min, the cooling time of paraffin wax to 30℃ is 194 minutes and 6 seconds, and under the condition of air flow 1.7L/min, the cooling time of paraffin wax to 30℃ is 186 minutes and 42 seconds. The nozzle diameter is 0.6mm, and the air flow rate is 0.9L/min, 1.1L/min, 1.3L/min, 1.5L/min and 1.7L/min, respectively.

ISSN: 2414-1895 DOI: 10.6919/ICJE.202304_9(4).0030

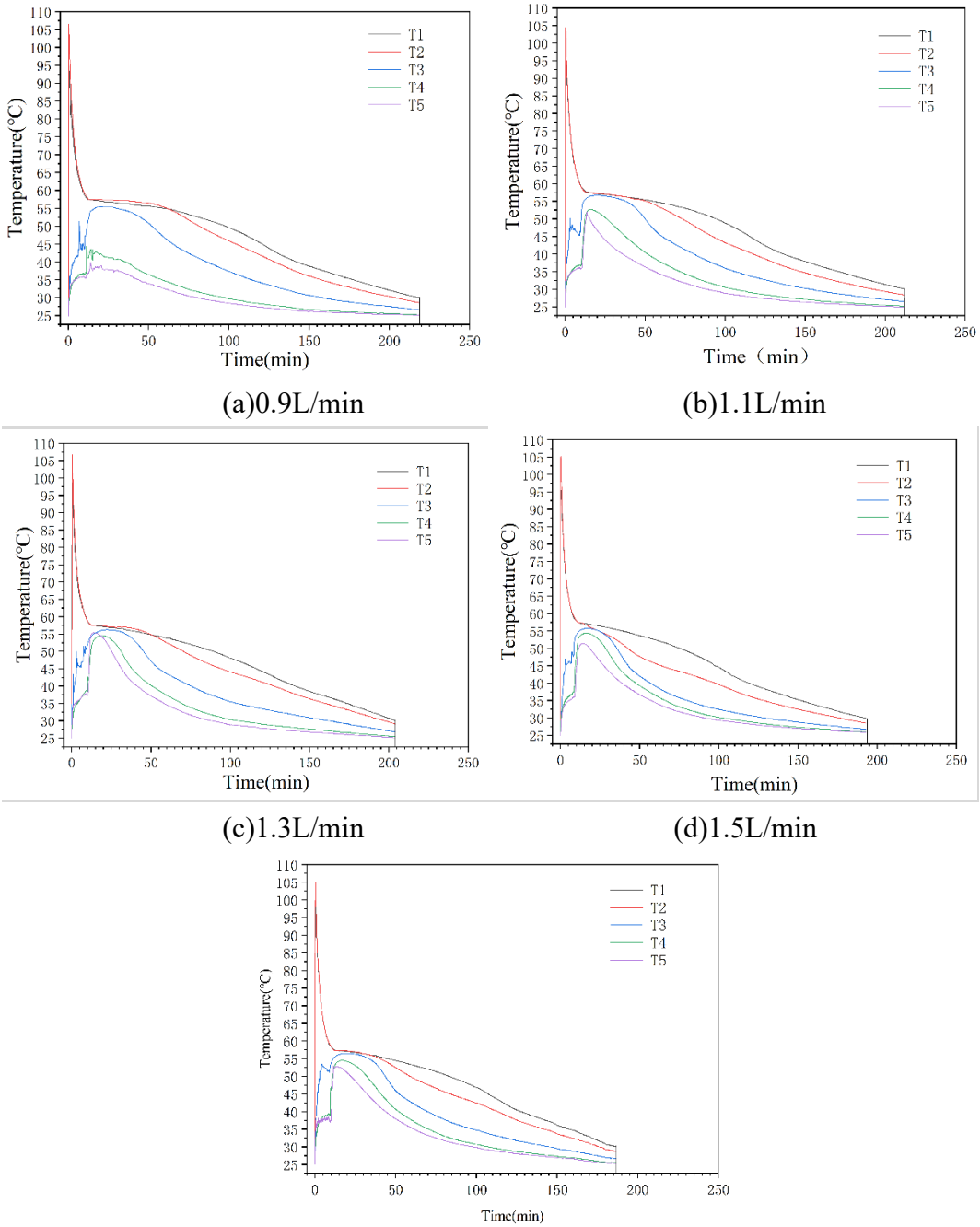

(a)0.9L/min (b)1.1L/min

(c)1.3L/min (d)1.5L/min

(e)1.7L/min

Fig 4. Temperature variation curve of 0.6mm nozzle paraffin

The nozzle diameter is 0.8mm, and the air flow rate is 0.9L/min, 1.1L/min, 1.3L/min, 1.5L/min and 1.7L/min respectively. Experimental data are shown in Figure 5. Under the condition of air flow of 0.9L/min, it takes 217 minutes and 51 seconds for paraffin to cool to 30℃; under the condition of air flow of 1.1L/min, it takes 208 minutes and 30 seconds for paraffin to cool to 30℃; under the condition of air flow of 1.3L/min, It takes 202 minutes and 52 seconds for the paraffin to cool to 30℃. Under the condition of 1.5L/min air flow, the cooling time of paraffin wax to 30℃ is 193 minutes, and under the condition of 1.7L/min air flow, the cooling time of paraffin wax to 30℃ is 184 minutes and 30 seconds.

ISSN: 2414-1895 DOI: 10.6919/ICJE.202304_9(4).0030

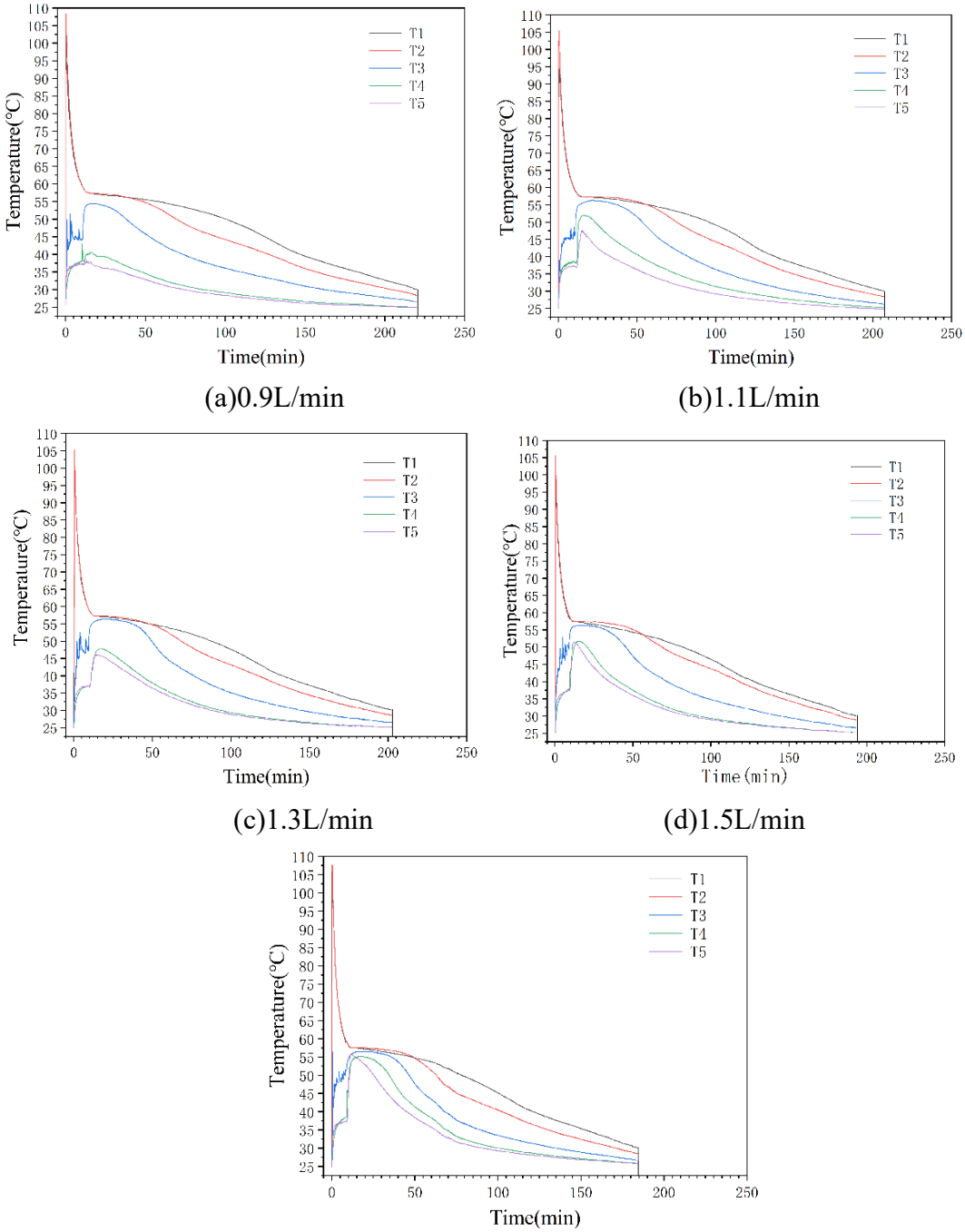

(a)0.9L/min (b)1.1L/min

(c)1.3L/min (d)1.5L/min

(e)1.7L/min

Fig 5. Temperature variation curve of 0.8mm nozzle paraffin

The nozzle diameter is 1.0mm, and the air flow rate is 0.9L/min, 1.1L/min, 1.3L/min, 1.5L/min and 1.7L/min, respectively. Experimental data are shown in Figure 6. Under the condition of air flow of 0.9L/min, the cooling time of paraffin wax to 30℃ is 217 minutes and 6 seconds; under the condition of air flow of 1.1L/min, the cooling time of paraffin wax to 30℃ is 203 minutes and 40 seconds; under the condition of air flow of 1.3L/min, It takes 198 minutes and 48 seconds for the paraffin to cool to 30℃. Under the condition of air flow 1.5L/min, the cooling time of paraffin wax to 30℃ is 191 minutes 51 seconds, and under the condition of air flow 1.7L/min, the cooling time of paraffin wax to 30℃ is 183 minutes 12 seconds.

ISSN: 2414-1895 DOI: 10.6919/ICJE.202304_9(4).0030

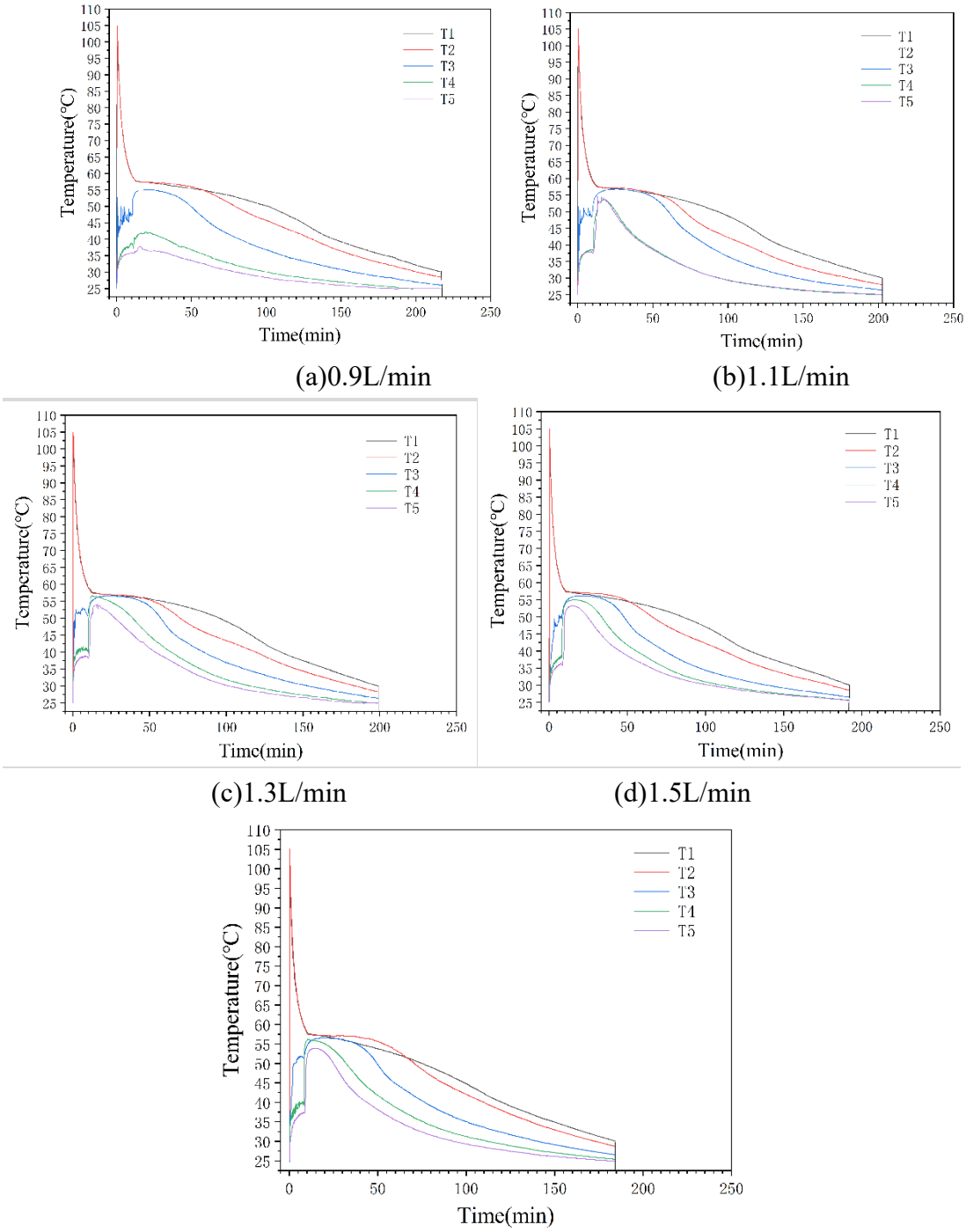

(a)0.9L/min (b)1.1L/min

(c)1.3L/min (d)1.5L/min

(e)1.7L/min

Fig 6. Temperature variation curve of 1.0mm nozzle paraffin

Under all the above conditions, the temperature change of PCM can be divided into three stages. First, the temperature of PCM drops sharply to near the melting point. Then, they remain constant near the melting point. Finally, the temperature of PCM is slowly reduced to 30°C. The first stage releases sensible heat of liquid PCM, the second stage releases latent heat of phase transition of PCM, and the third stage releases sensible heat of solid PCM. In Figure 1-5, the inlet of cooling gas reduced the temperature change of PCM in all three stages. In the second phase, the transformation time of PCM is shortened. In Figure 1 there is a relatively straight line segment, but in Figure 5 (e) this line segment is shortened.

ISSN: 2414-1895 DOI: 10.6919/ICJE.202304_9(4).0030

The experimental data show that the cooling temperature of paraffin decreases with the increase of air flow. Paraffin wax needs 243 to cool to 30℃ in its natural stateWhen the air flow rate of 1.0mm nozzle is 1.7L/min, the cooling time of paraffin wax is 184 minutes and 12s, which is shortened by 59 minutes and 21 seconds, and the cooling rate is increased by 24.36%. Due to the increase of cooling gas flow rate, the forced convection heat transfer between gas and PCM is enhanced, resulting in a decrease of cooling speed.

Under the same air flow and different nozzle diameters, the variation of cooling time tends to increase. When the nozzle diameter increases by 0.2mm, the maximum cooling time decrease occurs between 0.8mm and 1.0mm at the air flow rate of 1.1L/min, with a decrease of 2.4%, but most of them are below 1%. It is because increasing the nozzle diameter can increase the contact area between air and PCM, but also reduce the air flow rate, so increasing the nozzle diameter can significantly reduce the heat release time.

4.2 Solidification form of PCM

Figure 7 shows the paraffin solidification height at each gas flow rate with nozzle diameter of 0.4mm. It can be clearly seen that the height of PCM solidification measured is 40mm in the absence of gas inlet. With the increase of gas flow, the height of PCM in the accumulator also increases. FIG. 8 shows that at 1.7L/min, PCM fills the entire container, increasing its height by 275%. Due to gas intake, pores of different sizes will be formed in the interior of PCM during phase transition, and the internal volume of PCM is relatively loose, thus increasing. By cutting open the solidified PCM, it can be seen that the pores in the lower part of PCM are relatively small and dense, and larger and looser as the PCM goes up. The gas flow rate is fast when it first enters the accumulator, but the flow rate in the accumulator is subjected to friction resistance and the pressure it receives becomes smaller as it goes upward. The gas flow rate decreases and the bubbles become larger. Otherwise, the bubbles are easily blown during phase transition, so the pores above are large and loose. It can be seen that the condensed PCM has no impurities. During the test, only gas is passed into it but then comes out again. The PCM can be reused and its accumulator structure is simpler.

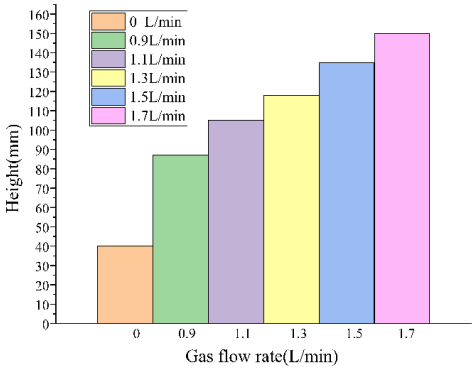

Fig 7. Height of paraffin solidification

4.3 Calculation and Analysis of Heat Transfer Power

In this experiment, the total enthalpy value of PCM is a constant value, but the temperature of PCM is measured from the pouring of PCM. From FIG. 2 to FIG. 6, it can be clearly seen that the highest temperature does not appear at the position at the moment of 0, but several seconds later. Since the initial temperature of the accumulator is room temperature at 25℃, which is higher than the initial temperature of PCM, heat conduction will occur at the beginning of pouring, which will reduce the temperature of PCM. However, the maximum temperature of 21 measurement conditions is about 105℃, and the error is within the acceptable range. This phenomenon will also occur in practical application. The total enthalpy value is calculated through equation (4), and the total enthalpy value and the condensation time measured in each experiment are substituted into Equation (5) to calculate the heat transfer power, as shown in Table 2.

ISSN: 2414-1895 DOI: 10.6919/ICJE.202304_9(4).0030

Table 2. Heat transfer power

Nozzle diameter mm	Gas flow rate L/min	Power W
0	0	4.97
0.4	0.9	5.45
0.4	1.1	5.66
0.4	1.3	5.87
0.4	1.5	6.20
0.4	1.7	6.45
0.6	0.9	5.51
0.6	1.1	5.70
0.6	1.3	5.93
0.6	1.5	6.23
0.6	1.7	6.48
0.8	0.9	5.55
0.8	1.1	5.80
0.8	1.3	5.96
0.8	1.5	6.26
0.8	1.7	6.55
1.0	0.9	5.67
1.0	1.1	5.94
1.0	1.3	6.08
1.0	1.5	6.30
1.0	1.7	6.60

As expected, the heat transfer power in the table increases with the gas flow rate under the nozzle of the same diameter, that is, the faster the heat transfer rate. In the experiment, the heat transfer power with gas entry is 31.99% higher than that without gas entry. The Origin polynomial fitting function is used to fit the gas flow rate, nozzle diameter and heat transfer power, and the fitting curve is shown in Figure 8.

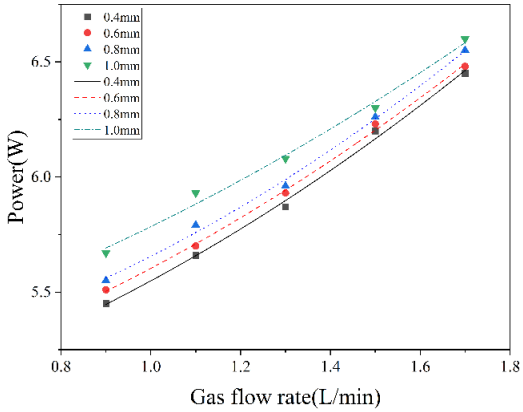

Fig 8. Power fitting curve

ISSN: 2414-1895 DOI: 10.6919/ICJE.202304_9(4).0030

As can be seen from FIG. 8, heat transfer power increases with the increase of gas flow under nozzles with the same diameter, and the trend of fitting curves of 0.4mm, 0.6mm and 0.8mm is very similar, but the fitting curves of 1.0mm are quite different. As mentioned above, under the gas flow rate of 1.1L/min, the cooling time of 0.8mm and 1.0mm has a large reduction, which is also reflected in the fitting curve, and the corresponding vertical spacing of power points has a large difference.

5. Summary

In this paper, K-type thermocouple and camera visualization experiments are used to study the heat release process of PCM in a direct contact vessel with gas as a heat transfer fluid, and the following conclusions are drawn.

(1) The cooling time of heated PCM decreases with the increase of incoming gas flow rate, and the cooling rate increases by 24.36%.

(2) Under the same air flow and different nozzle diameters, the cooling time has an increasing trend, but the increasing trend is not obvious, mostly below 1%.

(3) The volume of PCM increases after gas entry and solidification, and the volume increases with the increase of gas flow. When the gas flow rate is 1.7L/min, the volume increases by 275%.

(4) The heat transfer power increases with the increase of the inlet gas flow rate, and the heat transfer power increases by 31.99%.

(5) PCM can be directly reused without adding other substances, and the structure of the accumulator is simpler.

References

[1] Das N,Takata Y,Kohno M,et al.Melting of graphene based phase echange nanocomposites invertical latent heat thermal energy storage unit[J].Applied Thermal Engineering, 2016, 107:101-103.

[2] Motahar S,Nikkam N,Alemrajabi A A,et al.Experimental investigation on thermal and rheological properties of n-octadecane with dispersed TiO2 nanoparticles [J].International Communications in Heat and Mass Transfer,2014,59:68-74.

[3] Mao Q J,Li Y,Li G Q,et al. Study on the influence of tank structure and fin configuration on heat transfer performance of phase change thermal storage system[J]. Energy,2021, 235: 121 382.

[4] Stritih U. An experimental study of enhanced heat transfer in rectangular PCM thermal storage[J]. International Journal of Heat and Mass Transfer, 2004, 47(12-13): 2841 - 2847.

[5] Kaizawa a, Kamano h,Kawai a,et al. Thermal and flow behaviors in heat transportation container using phase change material[J]. Energy Conversion and Management, 2007, 49 (4):689-760.

[6] Nomura t,Tsubota m, Sagara a,et al. Performance analysis of heat storage of direct-contact heat exchanger with phase- change material[J]. Applied Thermal Engineering, 2013, 58: 108-113.

[7] Viktoria m, Bo h, Fredrik s,Direct contact PCM-water cold storage[J].Appl Energy,2010,87(8):2652-2659.

[8] Guo s p,liu q b,Zhao j,et al.Mobilized thermal energy storage: Materials, containers and economic evaluation[J]. Energy Conversion and Management,2018,177:315- 329.

[9] Gao l h, Zhao j,An q s,et al. Experiments on thermal performance of erythritol/expanded graphite in a direct contact thermal energy storage container[J]. Applied Thermal Engineering,2016,113:858-866.

[10] Huang J w,Zheng G f,Li M,et al. Assessing the effects of fluids flow on heat transfer performance in direct contact heat transfer process through EMD-LSSVM model: An experimental study[J]. Applied Thermal Engineering,2021,189.

[11] He s q, Wang w l, Wei l h, et al.Heat transfer enhancement and melting behavior of phase change material in a direct-contact thermal energy storage container[J].Journal of Energy Storage, 2020,31:101665.

[12] Belusko M,Sheoran S,Bruno F.Direct contact phase change material thermal energy storage[J]. High Temperature Thermal Storage Systems Using Phase Change Materials, 2018:7-37.

ISSN: 2414-1895 DOI: 10.6919/ICJE.202304_9(4).0030

[13] Wang W L, Li h l, Guo s p, et al.Numerical simulation study on discharging process of the direct-contact phase change energy storage system[J].Applied Energy, 2015,150:61-68.

[14] Sven k, Tobias T , Patrick D,et al.Determination of heat transfer coefficients in direct contact latent heat storage systems[J]. Applied Thermal Engineering,2018,145:71-79.